Weathering-independent differentiation of microplastic polymers by reflectance IR spectrometry and pattern recognition

Borja Ferreiro, Jose M. Andrade [*], Carlota Paz-Quintáns, Verónica Fernández-González, Purificación López-Mahía, Soledad Muniategui

Grupo Química Analítica Aplicada (QANAP), Instituto Universitario de Medio Ambiente (IUMA), Universidade da Coruña, 15071 A Coruña, Spain

A B S T R A C T

The presence and effects of microplastics in the environment is being continuously studied, so the need for a reliable approach to ascertain the polymer/s constituting them has increased. To characterize them, infrared (IR) spectrometry is commonly applied, either reflectance or attenuated total reflectance (ATR). A common problem when considering field samples is their weathering and biofouling, which modify their spectra. Hence, relying on spectral matching between the unknown spectrum and spectral databases is largely defective. In this paper, the use of IR spectra combined with pattern recognition techniques (principal components analysis, classification and regression trees and support vector classification) is explored first time to identify a collection of typical polymers regardless of their ageing. Results show that it is possible to identify them using a reduced suite of spectral wavenumbers with coherent chemical meaning. The models were validated using two datasets containing artificially weathered polymers and field samples.

1. Introduction

Plastics constitute a durable, lightweight, and versatile family of materials from which an immense variety of products are created. Their applications range from food packaging to sports, electronics, construction and transport. Currently, plastics are required in so many industrial fields that they became an indispensable material for many commodities and complex products (cars, planes, etc.), with their global production reaching 367 million tonnes in 2020, of which Europe accounted for 55 million tonnes (Mt) (PlasticEurope, 2021). Polypropylene and polyethylene are the most demanded polymers (19.7 % PP, 17.4 % LDPE, 12.9 % HDPE), followed by PVC (9.6 %) and PET (8.4 %), mostly for packaging. China accounts for the highest plastic consumption and production, with up to 32 % of the World's plastic production in 2020 (PlasticEurope, 2021).

A consequence of the massive use and inadequate recovery and recycling of plastics is that they have become one of the most ubiquitous anthropogenic contaminants in the World's environments. They have been found in soil (Bläsing and Amelung, 2018), airborne particles (Prata, 2018), water (Koelmans et al., 2019) and food (Van Cauwenberghe and Janssen, 2014). However, the problem is specially serious on aquatic environments (Jiang, 2018). It was estimated that in

2018 alone 5.5 to 14.5 Mt entered the oceans (Wayman and Niemann, 2021) and, as a consequence, seas and oceans have plastic debris both at their surface and seabed worldwide. There are many regions affected by this kind of pollution, even in deep sea trenches (Chiba et al., 2018). The most affected zone is the North Pacific area (Howell et al., 2012) as oceanic currents drag the plastic debris to this zone, generating plastic 'fields' swirling in the oceanic surface. This has been demonstrated to have a detrimental effect on different species of marine flora and fauna (Coffin et al., 2019; Lamb et al., 2018; Markic et al., 2020; Wang et al., 2016; Wilcox et al., 2018; Young et al., 2009).

Microplastics (MPs) can be defined as '*any solid plastic particle insoluble in water with any dimension between 1μm and 1 mm*', being larger particles –between 1 mm and 5 mm- '*large microplastics*' (ISO, 2020). The smaller sizes in particular, along with nanoplastics, can enter the trophic chain through plankton (Botterell et al., 2019), fish (Bellas et al., 2016) and other marine species by ingestion (Jiang, 2018), and it is common to find microplastics in the digestive system of different aquatic species (Bellas et al., 2016; Compa et al., 2018). This fact, along with an improved capacity to adsorb other contaminants in comparison with meso- and macroplastics, is known to have detrimental effects (Gewert et al., 2015), which might affect human health through ingestion of –as a matter of example- shellfish (Van Cauwenberghe and Janssen, 2014),

fish (Battaglia et al., 2016; Bellas et al., 2016) and table salt (Iñiguez et al., 2017). In fact, in recent studies, plastics have been found in human blood and lung tissue (Jenner et al., 2022; Leslie et al., 2022).

Therefore, a successful identification of the polymers found in the environment is of utmost importance to evaluate their distribution, origin, or subsequent behaviour there. This can be done using different analytical techniques, a common one being vibrational spectrometry. Its speed, high selectivity, and low demand of sample quantity make it a suitable technique for MPs analysis. Besides, it is easily combined with microscopic techniques and attenuated total reflectance (ATR) accessories. Although ATR spectrometry is well suited for measuring big and medium particles (let's say >500 µm) it is not suited for smaller ones. Here it is where reflectance gains momentum and overcome the ATR limitations as it does not need direct contact between the sample and the IR focusing device. Two nice reports on the use and limitations of various types of IR spectrometry are those from Veerasingam et al. (2021) –that includes some interpretation of spectral bands- and Primpke et al. (2020) –that included a comparison with other analytical methodologies-.

Irrespectively of the analytical measuring technique, there are many physical, biological and chemical processes that plastics undergo while in the environment (e.g., mechanical erosion, photodegradation due to the UV light and biological colonization). They can modify the original polymers by breaking their molecules into smaller ones, oxidizing their chains (usually due to chain attack by UV-originated radicals), giving rise to/modifying oxygenated functional groups (carboxylic acids, ketones, peroxides, etc.), crosslinking alterations, changing crystallinity, etc. Many times this leads to smaller plastic fragments. All these effects are known collectively as 'weathering' and more details can be found elsewhere (Göpferich, 1996; Gewert et al., 2015; Raddadi and Fava, 2019; Chamas et al., 2020; Ali et al., 2021; Zhang et al., 2021). The final consequence is that weathering alters the surface of the (micro)plastics and, so, their spectra. Many IR spectral bands evolve with weathering, some others appear, others broaden and/or overlap with neighbouring signals, etc. All this hinders the interpretation of the spectra. Many practitioners rely on spectral matching between the unknown spectrum and spectral databases to account for polymer identification. However, often the latter cannot properly match the former due to the aforementioned problems, as reported frequently; e.g., Fernández-González et al. (2021a) and Mecozzi et al. (2016).

A complete relation of the evolution of each of the polymers used in this work is out of the scope of this paper and only some general details will be given. Interested readers are kindly forwarded to the references cited next, and those referred to therein. The most relevant changes observed in the spectra were compatible with damages caused by the UV radiation that gave rise to chain attacks by radicals (Norris-type reactions). A general introduction to those modifications was presented by Gewert et al. (2015). Specific changes on the spectra and surface of the five most common packaging polymers –LDPE, HDPE, PS, PP and PET- and PA6.6 were studied previously (Fernández-González et al., 2021a, 2021b). In the former paper, a table resumed which bands increased or decreased with time, per plastic. Also, dramatic changes on the polymeric structure (leakage of Cl atoms and appearance of C=C bonds) were reported for weathered PVC particles (Fernández-González et al., 2022), which might explain the usually low reports of PVC microplastics in environmental samples. Particular details can be found elsewhere for PET (Gok et al., 2019; Oreski and Wallner, 2005; Renner et al., 2017; Venkatachalam et al., 2012), LDPE (Brandon et al., 2016; Hirsch et al., 2017; Luo et al., 2020), PC (Shi et al., 2021), PP (Brandon et al., 2016; ter Halle et al., 2017), and PS (Yousif and Haddad, 2013).

A natural way to reduce this problem is to include spectra of weathered polymers into the databases (Fernández-González et al., 2021a). In this sense, a low-cost weathering system was proposed recently to resemble natural conditions (Andrade et al., 2019) and standardize this task. The need for complete databases and the risk of relying on current correlation coefficients to identify unknown particles

were presented by Mecozzi et al. (2016) and they proposed a suite of three similarity indexes and the use of independent components analysis to search the database.

Another novel and totally different route to mitigate this problem is explored in this work using unsupervised chemometric pattern recognition. The main objective of this paper is to explore a new way to get rid of the spectral information related to the weathering processes of the materials constituting the MPs. If so, the remaining spectral characteristics, which in essence will not be affected by weathering, would simplify the identification of the polymers and, therefore, open up new possibilities for MPs studies and environmental monitoring. It is worth noting that this working hypothesis does not correspond to typical pattern recognition studies where the most important patterns (linked to the first statistical factors that explain most of the variance into the spectral data) are used to, precisely, visualize the sets of samples. Here we look in the other way around; i.e., how the influence of weathering on the spectra – which constitute their principal source of variation - can be avoided and, so, weathered and unweathered specimens of a polymer appear close together after a statistical study (e.g. in a given plot of the samples). As a referee pointed out, a similar though conceptually different approach would be to look for parameters not evolving with time, but such an approach was not considered in this work.

2. Experimental

2.1. Samples

The polymers used throughout this study were provided by the Universität of Bayreuth (Germany), within the framework of the JPI-Oceans-funded BASEMAN project. They were fabricated with the lowest possible amount of additives. Two sample forms were studied: powder (average size ca. 300 µm) and pellets (average size ca. 3 mm), more details can be found in the Supplementary material.

Small quantities (10–20 g) of all polymers were aged for 10 weeks in a dedicated ad-hoc weathering system designed for standardizing the weathering of MPs at geographical medium latitude (Andrade et al., 2019). Aliquots were either submerged in seawater to simulate weathering in the superficial oceanic layer or kept dry to simulate weathering at the shoreline (e.g., upper part of beaches and dunes). An aliquot of each polymer was withdrawn weekly from each weathering container and measured by ATR and micro reflectance infrared spectrometry. The experimental weathering conditions and related details can be found elsewhere (Andrade et al., 2019). Fig. SM1 (Supplementary material) exemplifies the reflectance spectra obtained for the pelletized and powdered samples.

In the present work, the pristine (*as received*) and ten aliquots withdrawn from the weathering system weekly were considered. Half the samples, the odd ones, were employed to calibrate the models whereas the even were used for validation. In addition a second field dataset composed of 67 field plastic fragments collected from three Mediterranean beaches studied previously (León et al., 2019) was used to test the models under field monitoring conditions.

2.2. Equipment

A Spectrum 400 FT-IR Perkin-Elmer spectrometer coupled with a Perkin Elmer IR Spotlight 200i microscope and a horizontal one-bounce diamond ATR (Miracle, Pike, USA) were employed. Each particle was measured twice (changing the position of the pellet) and the resulting spectra were averaged. The MIPIR (minimum information for publication of IR-related data on MPs characterization (Andrade et al., 2020)) experimental setup was: resolution: 4 cm^{-1}; number of scans: 200; spectral range: 3500–600 cm^{-1}; background recording before measuring each particle; aperture: 100 µm (adjusted to smaller apertures whenever the granule was smaller); apodization: Beer-Norton, strong; spectral processing: multipoint baseline correction plus

normalization 10 % plus Kubelka-Munk (for pellets), and multipoint baseline correction plus Kramers-Kronig (for powders). ATR spectra were corrected for depth penetration. The sample form affects the required spectral processing due to the different interaction the surface of the granule has with the IR beam. For pellets the surface selected for measurements was mostly flat, making the reflection mostly specular. For powders, however, the reflection is mostly diffuse, due to the irregularities of the powder grains.

Reflectance instead of transmittance was considered because the former is very common to deal with MPs characterization; mainly, attenuated total reflectance, ATR, but also specular and diffuse reflectance (Fernández-González et al., 2021b). Reflectance spectra do not depend in essence on particle thickness and can be applied straightforwardly. On the other hand, as reflectance characterizes the surface of the particles it is affected by polymer ageing and, so, the studies presented in this paper are worth of interest for routine use.

2.3. Software

The multivariate statistical software employed throughout was GenEx7 (MultiD Analysis AB, Göteborg, Sweden), Matlab's PLS Toolbox (Eigenvector Co, USA) and Orange (University of Ljubljana, Slovenia).

2.4. Chemometric tools

The evolution of IR spectra during weathering makes this source of variance (statistical information) dominate the distribution of the samples in multivariate analyses. This difficults or impedes the correct assignation of a material to a type of polymer. Such an information is what it is expected to avoid here.

The three chemometric techniques applied in this paper are depicted briefly in the Supplementary material. They are principal components analysis (PCA), classification and regression trees (CART) and support vectors machine (SVM). They correspond to standard algorithms available in any chemometric statistical package, no implementation changes have been done. Therefore, the explanations refer to the conceptual bases of the techniques, without going into mathematical details (which are available in the references given therein). Non skilled readers are kindly encouraged to review the Supplementary material for the basic meaning of the terms scores and loadings as they are used throughout the next sections. They also constitute the basis of two variable selection approaches.

The major output of a PCA study is a set of combinations of variables, each of which is a principal component, PC (see Supplementary material for a simplified explanation on how they are calculated and interpreted from a chemical viewpoint). To avoid confusion with polycarbonate (whose acronym is also PC) references to the principal components will be always associated to an ordinal (i.e., the number of the principal component under discussion; e.g. PC4), or to the plural form, PCs.

SVM was performed using a reduced set of variables derived from the most relevant PCA loadings. In particular, those from the PCs that differentiated the most among the polymers. The data pretreatment for the SVM models that used micro reflectance spectra was the same as for the PCA model from which the variables were selected (automatic baseline correction plus first derivative). The data pretreatment for SVM models developed with ATR spectra required baseline correction (automatic weighted least squares, 2nd order), normalization (area = 1), and standard normal variate (SNV).

For the CART models no pretreatment was applied, but the spectra were reduced to the 1800–600 cm^{-1} range, in order to avoid variables without real information (atmospheric CO_2 peaks, baseline and noise) and to reduce the computational burden.

To evaluate the performance of the models a series of straightforward statistics can be calculated: the *ratio of false positives* (calculated as (false positives) / (true negatives + false positives)); and the *ratio of false negatives*, calculated as (false negatives) / (true positives + false

negatives). Also, the Mathews' Correlation coefficient (MCC) was calculated to accurately summarize the behaviour of the models (Cuadros-Rodríguez et al., 2016), following the equation below:

$$MCC = \frac{(TP*TN) - (FP*FN)}{\sqrt{(TP + FP)*(TP + FN)*(TN + FP)*(TN + FN)}}$$

where TP is the number of true positives in the sample, TN the number of true negatives, FP the number of false positives and FN the number of false negatives. A perfect model would yield a MCC value of 1. In all models, the criterion used to assign a sample to a group was the 'most probable' (i.e., the sample is included in the group to which it shows the highest probability).

3. Results and discussions

To simplify the discussions and comparisons among the studies, the results for the pelletized form of the polymers are presented first for seawater and second for dry conditions, for both the micro reflectance and ATR measurements, each. Then, those for the powder form will be given in the same order. The results are presented in the following order: 1st, the PCA study (scores and loadings), with the identification and interpretation of the most relevant loadings; 2nd, dynamic PCA; 3rd, PCA using only the variables associated to the most relevant loadings; 4th, SVM model; and 5th, CART model.

The chemical interpretation of the loadings is presented graphically for the sake of simplicity and to avoid repetitive discussions. Specific details on the interpretation of the IR spectra for the different polymers and their functional groups can be found in some previous works; for example, those from Arrieta et al. (2013), Brandon et al. (2016), Mecozzi et al. (2016) -although they focused on the most relevant bands to identify the polymers-, Tiwari et al. (2019), Vasanthan (2012), Veerasingam et al. (2021) and the exhaustive recopilation of Jung et al. (2018).

In addition to the spectral processing detailed in Section 2.2, the data pretreatment for the PCA was: automatic baseline correction (using a second order polynomial function) plus normalization (total area = 1) plus mean centring. The pretreatment for powders measured by micro reflectance was: automatic baseline correction plus first derivative. These treatments were selected after several preliminary trials as they yielded the best groups of samples.

3.1. Pellets weathered in seawater

The PCA carried out on the micro reflectance spectra of the pellets weathered in seawater conditions revealed that they could be differentiated nicely using the PC1-PC4-PC6 subspace (56.2 % explained variance), see Fig. 1a. PC2, PC3 and PC5 did not differentiate them because even though they could group some polymers the others led to widely dispersed scores (likely, due to weathering), yielding overlaps between the groups and impeding their separation.

PC1 (39.5 % explained information) in essence opposes PC, PET and PMMA (negative scores) to the other polymers (with positive or close-to-zero scores), the former being the polymers with the most complex chemical structures. Fig. 2 shows that the variables contributing more to this factor are clearly associated to HDPE and LDPE, with positive loadings, and also related with highest positive scores in PC1. The most important negative loadings characterize PC, PET and PMMA.

PC4 (11.2 % explained variance) separates PA (negative scores) and PS (positive scores, Fig. 1b). The loadings are mostly related to PA (Fig. 2, negative loadings) but for a band at 698 cm^{-1}, which can be attributed mainly to PS due to its aromatic nature and positive loading.

PC6 (5.5 % explained information) separates basically PET (characterized by the most negative scores, Fig. 1b; and negative loadings, Fig. 2) from PP plus PMMA (with positive scores, Fig. 1b, and positive loadings associated to the paraffinic characteristics of PP and PMMA,
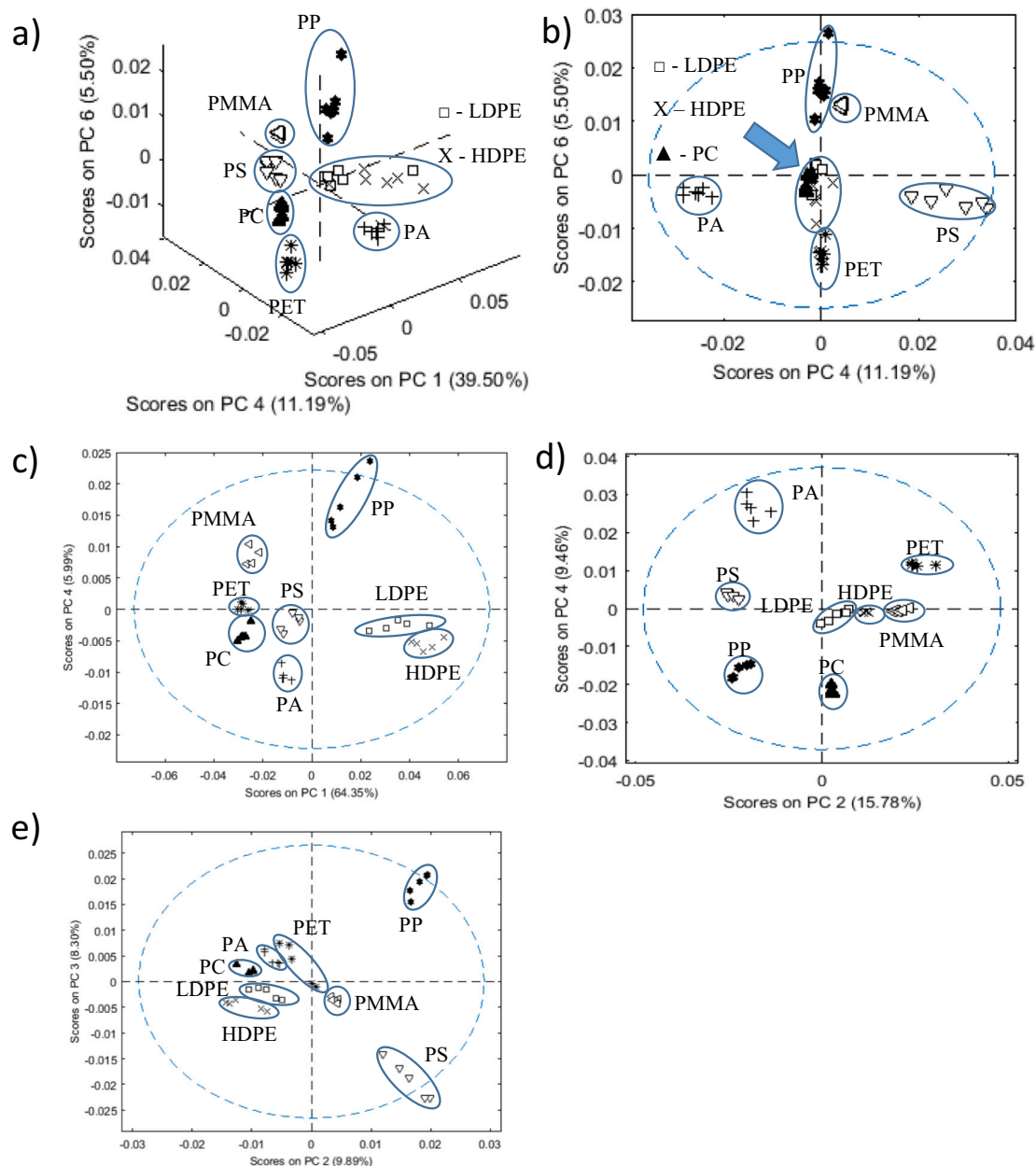
Fig. 1. Representation of the most relevant principal component subspaces to identify the groups of polymers. Seawater-aged pellets measured by micro reflectance (a) and (b), and by ATR (c). Dry-aged pellets measured by micro reflectance (d) and by ATR (e).

Fig. 2).

Using dynamic PCA it was possible to reduce the overall number of wavenumbers from 3400 to 10 and they still allowed visualizing the groups of polymers: 3455, 3024, 2918, 1775, 1631, 1268, 1262, 1230, 1156, and 706 cm^{-1}. All the variables are coherent with those illustrated in the loadings figures (Fig. 2, and Supplementary material), with the exception of 3455 and 3024 cm^{-1}, that are associated with the humidity of the samples (Brandon et al., 2016).

When the variables associated with the maxima of the loadings were used (only 11 wavenumbers corresponding to the peaks labelled in Fig. 2) to develop a dedicated PCA the groups of polymers could also be differentiated. SVM models considering these wavenumbers yielded satisfactory classifications, with only partially erroneous models when considering HDPE and LDPE. Fig. 3a exemplifies the separation of HDPE in a model, where the similarity between HDPE and LDPE is clear (indeed, they have minor spectral differences). Fig. 3b exemplifies the optimization of the cost and gamma parameters required to get the SVM model.

Finally, CART studies required only 7 divisions (14 branches) to successfully separate the polymers (Fig. 4a). This implied that only 7 variables were required (i.e., 1797, 1749, 1663, 1602, 1512, 1475 and 1268 cm^{-1}), whose interpretation agrees quite well with the previous relevant vector loadings (the C—O stretching, N—H bending plus C—N stretching, and the C=O typical functional groups can be seen rather clearly here).

When the ATR spectra were considered, the polymers could be differentiated using just two PCs: PC1 and PC4 (70.34 % explained variance, Fig. 1c). PC2 and PC3 could not separate HDPE and LDPE. In this study the 4000 to 3000 cm^{-1} region (mostly attributed to water) was excluded, as well as a PMMA sample, due to its anomalous behaviour. It is worth noting that PC1 and PC4 were also required when using the micro reflectance dataset above.

PC1 (64.35 % explained information) in essence opposes the most 'simple' polymers HDPE, LDPE and PP (positive scores, Fig. 1c,
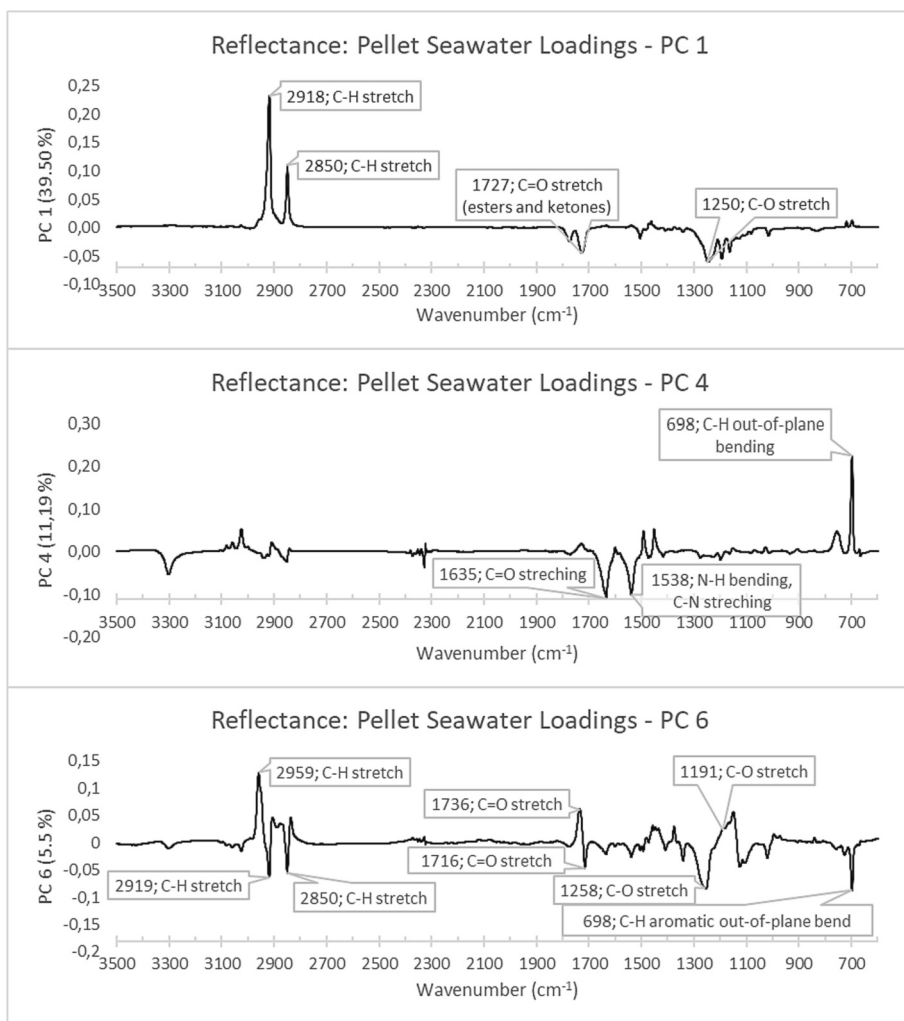
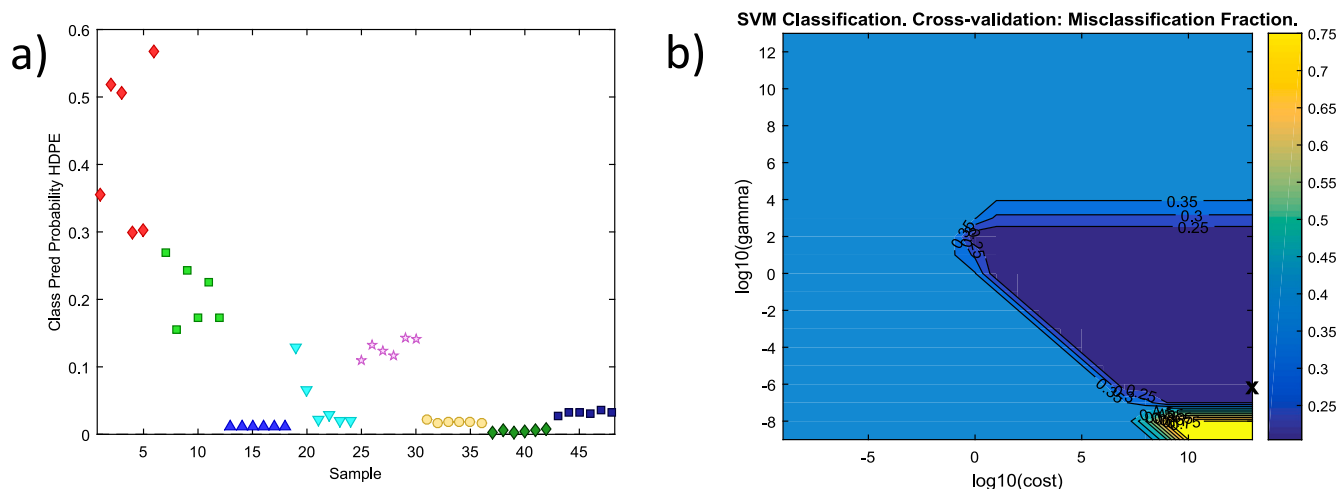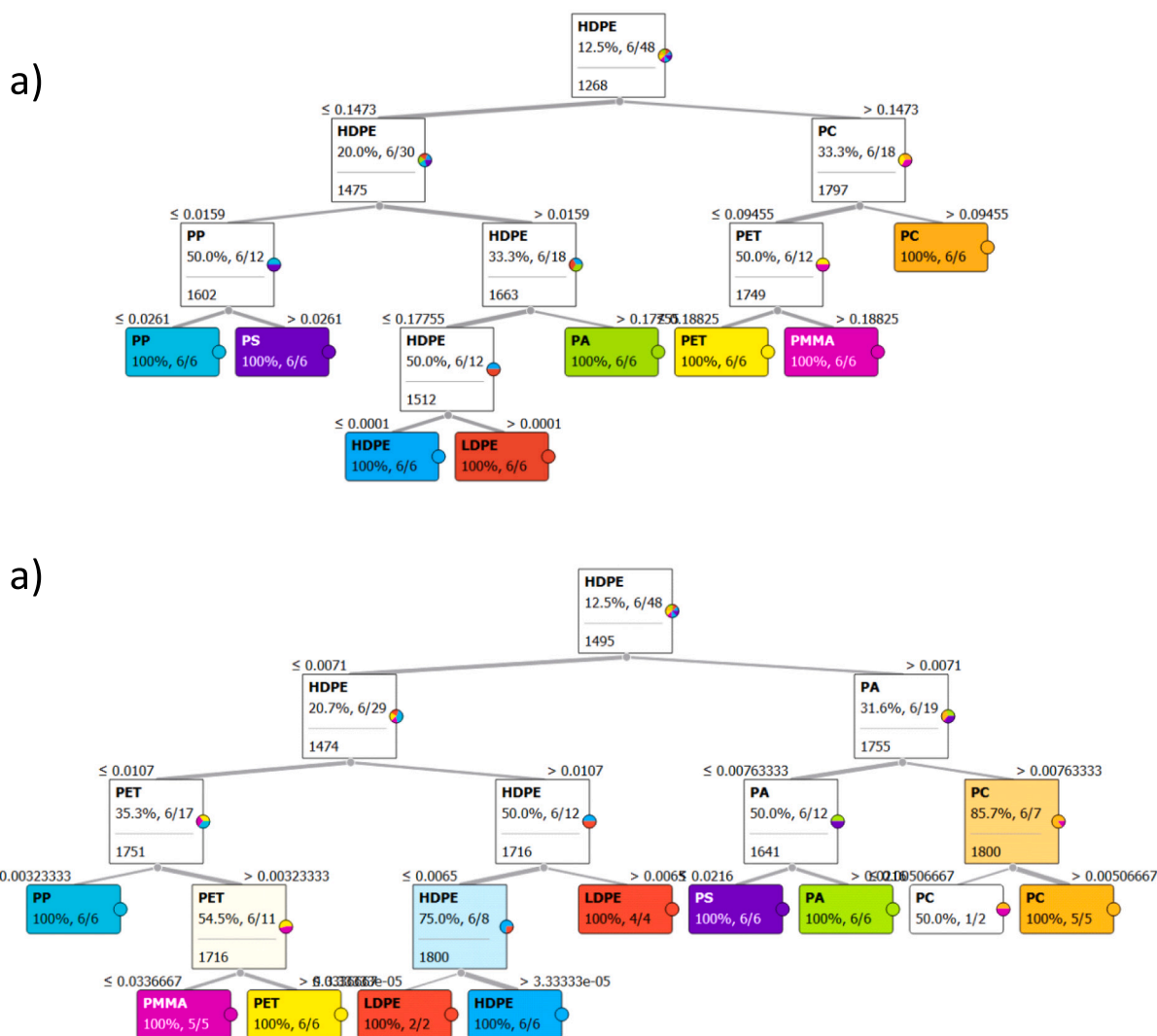**Fig. 2.** Seawater-aged pellets, micro reflectance loadings.

Fig. 3. a) Example of a SVM classification model, corresponding to pelletized HDPE aged in seawater and measured by micro reflectance IR spectrometry. b) Optimization of the cost and gamma parameters (the optimal value is marked with an X at the low, right corner).

characterized by the most relevant positive loadings in PC1, Fig. 5) to the other polymers, mainly PC, PET and PMMA, described by negative loadings (Fig. 5).

PC4 (6 % explained variance) separates mostly PA6.6, with negative

scores and negative loadings, from PP which has positive scores and positive loadings (Figs. 1c and 5, respectively). The maximum loadings agree with characteristic spectral peaks for these polymers.

The use of dynamic PCA reduced the variables needed to keep the

Fig. 4. Pellets aged in seawater, schematic representation of the CART decision tree obtained from the micro reflectance (a) and ATR (b) measurements. The final groups (each in a different colour) are 100 % homogeneous. The values at the bottom of the decision boxes correspond to the discriminating wavelength whereas the values over the boxes are the absorbance of the wavenumber that separates the branches (e.g., in the first node, if the absorbance at 1268 cm^{-1} is lower than or equal to 0.1473 a.u. the polymer may be HDPE, LDPE, PA, PP or PS).

polymer groups to 10 wavenumbers, at: 2959, 2847, 1736, 1544, 1420, 827, 872, 702, 699 and 688 cm^{-1}.

When the variables associated to the maximum loadings of both factors were used (6 in total), the groups of polymers could also be differentiated, with the exception of a PMMA outlying sample (as noted above). Application of SVM considering only those wavenumbers yielded good separations, with the exception of some HDPE and PS samples.

Finally, CART required only 9 divisions (18 branches) to get a good separation of the polymers (Fig. 4b). The 7 variables required for the sequential decisions were 1800 (twice), 1755, 1751, 1716 (twice), 1495, 1474 and 1641 cm^{-1}, whose general interpretation (CH$_2$ bending and C=O stretching) mostly agrees with the regions selected by dynamic-PCA (but for the 3000–2800 cm^{-1} spectral region, not included in CART, as explained above).

However, the classification is not as nice as that derived from micro reflectance measurements. The final groups for PP, PET, HDPE, PS and PA are 100 % homogeneous and form differentiated groups. However, LDPE needed two criteria (at 1716 and 1800 cm^{-1}) to be differentiated from HDPE and a PC sample mixes with another PMMA one, although the other pellets of these polymers became well separated.

3.2. Pellets weathered under dry conditions

When micro reflectance measurements were made, the factors that lead to the best differentiation among polymers were PC2 and PC4 (25.2 % explained information, Fig. 1d).

PC2 (15.8 % explained variance) differentiates PMMA and PET (positive scores) from PP, PS and PA (negative scores). Fig. SM2 (Supplementary material) shows the most relevant loadings defining this factor. PMMA and PET became characterized by their ester characteristics (the most positive loadings) while PA, PS and PP were characterized by negative loadings. No distinctive loadings can be attributed to PP, but for the typical CH stretching at ca. 2850 and 2950 cm^{-1}.

PC4 (9.5 % explained variance) is dominated by the Amide II band (NH monosubstituted amide bending plus the CN stretching) and differentiates basically PA (positive scores and positive loadings) from PC and PP (negative scores and their associated loadings, Fig. SM2). The negative loadings seem mostly linked to PC as the PP characteristics (stretching and bending of the CH bonds) cannot be seen, probably, masked by the CH bonds of PA6.6.

Using dynamic PCA the overall number of wavenumbers needed to visualize the groups of polymers got reduced from 2900 to 15 variables.
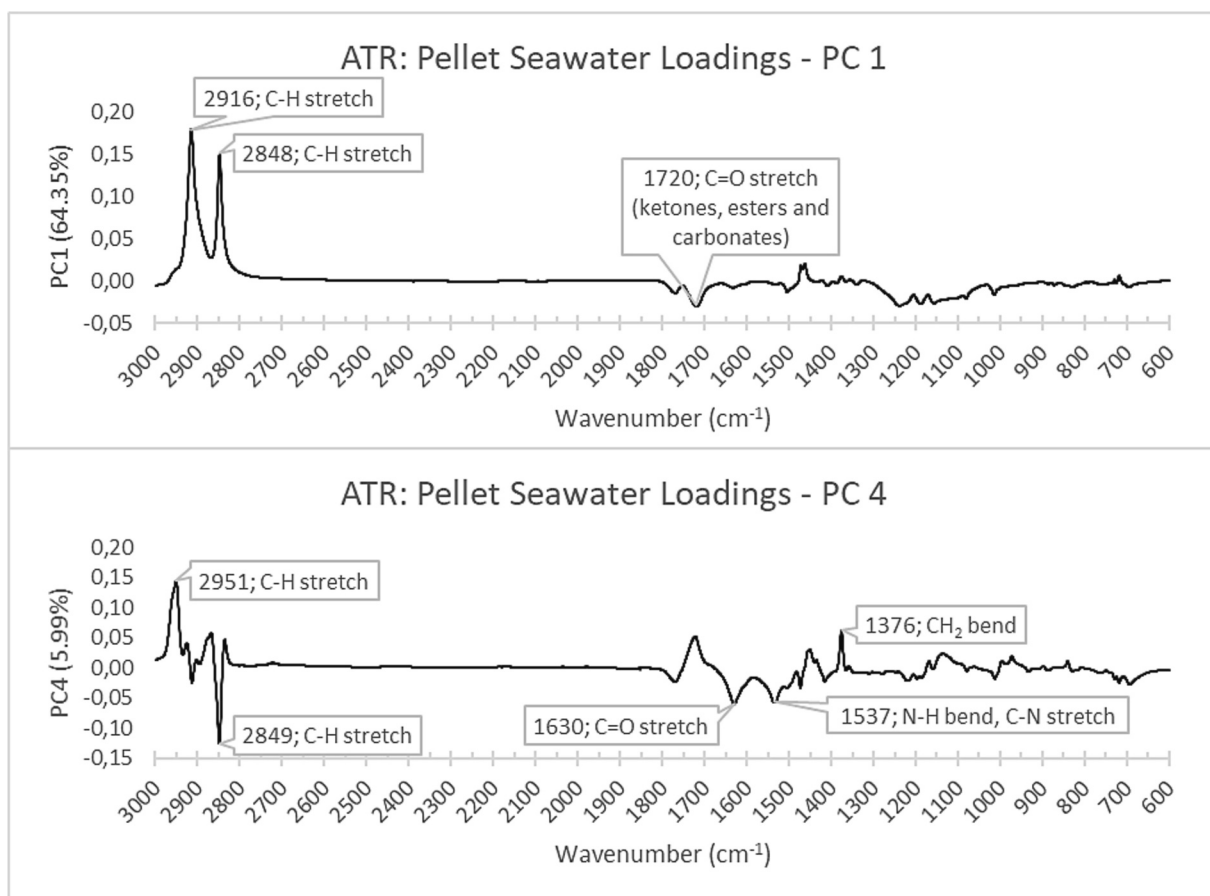
Fig. 5. Seawater-aged pellets, ATR loadings.

These were: 3457–3455, 2918, 1917, 1775, 1732, 1731, 1636–1634, 1269, 1268, 698, and 697 cm^{-1} wavenumbers.

When the 12 variables associated to the most relevant loadings of the principal components were used to perform a dedicated PCA the groups of polymers could still be differentiated. Using SVM, however, it was not possible to categorize the HDPE and LDPE samples. Finally, CART required 10 divisions (20 branches) to successfully separate the polymers (Fig. SM3), using only 9 variables (i.e., 1800 (twice), 1795, 1740, 1677, 1651, 1474, 1468, 1465 and 600 cm^{-1}).

For ATR spectra, the factors that differentiated the polymers best were PC2 and PC3 (18.2 % explained information, Fig. 1e). PC1 could not separate several polymers despite it takes account of more information (likely related to ageing). This result is similar to that with reflectance data above. However, the interpretation of the loadings is a bit more complicated here.

Positive scores and loadings in PC2 (9.89 % explained variance) differentiated clearly PP and PS from the other polymers. The most important positive loadings were linked to PS and PP (the peaks at 2950 and 1452 cm^{-1}) (Fig. SM4). The peaks at 2950 and 1452 related to PP, whereas the others are characteristic of PS. The most relevant negative loadings relate to the C—H stretching of HDPE and LDPE, whose samples outstand in the negative scores. The loading at 1720 cm^{-1} points towards the C=O groups of PC, PA and PET.

PC3 (8.30 % explained variance) separates PP from PS (Fig. 1e), whose scores in PC2 are almost the same. It also helps differentiating LDPE, HDPE and PMMA from PC, PA and PET. Here, it is difficult to assign loadings to specific monomers. The most important loadings relate to C—H stretching, CH$_2$ bending, C—H bending and aromatic out-of-plane bending (see Fig. SM4).

With the use of dynamic PCA the number of variables can be reduced

to only 4, still with a nice polymer differentiation: 2925 and 2924 cm^{-1} (C—H stretch) and 1714 and 1713 cm^{-1} (mostly C=O bands).

When the variables associated only to the maximum loadings (positive and negative) were used (7 in total) to carry out a PCA, the groups of polymers were still differentiated. When SVM was applied to those variables it was possible to visualize several groups of polymers, but LDPE and PS offered unsatisfactory results.

Finally, CART required only 8 divisions (16 branches) to successfully separate the polymers (Fig. SM5) employing 8 variables (i.e., 1800, 1752, 1733, 1507, 1496, 1474, 1456 and 1378 cm^{-1}).

3.3. Powder aged in seawater

The typical PC1-PC2-PC3 scores subspace (51.9 % explained variance) is adequate to separate the polymers when their powders are weathered in seawater and measured by micro reflectance spectrometry (Fig. 6a and b).

PC1 (21.4 % variance) is devoted to differentiate the PS samples (the most negative scores, Fig. 6a and b). It is not surprising thus that the most remarkable loadings in this factor are associated to PS (Fig. SM6); even the typical four peaks of similar intensity that characterize the typical monosubstituted aromatic pattern between 2000 and 1700 cm^{-1} can be seen.

PC2 opposes the 'simplest' hydrocarbon structures of PP, HDPE and LDPE (negative scores) to the other polymers (which contain heteroatoms and aromatic and more complex monomeric structures), in particular to PS (highest positive scores and whose bands can be linked to the largest positive loadings, Fig. SM6). The most relevant positive loadings are associated to –likely- the more linear structures: CH$_2$ bending and rocking.
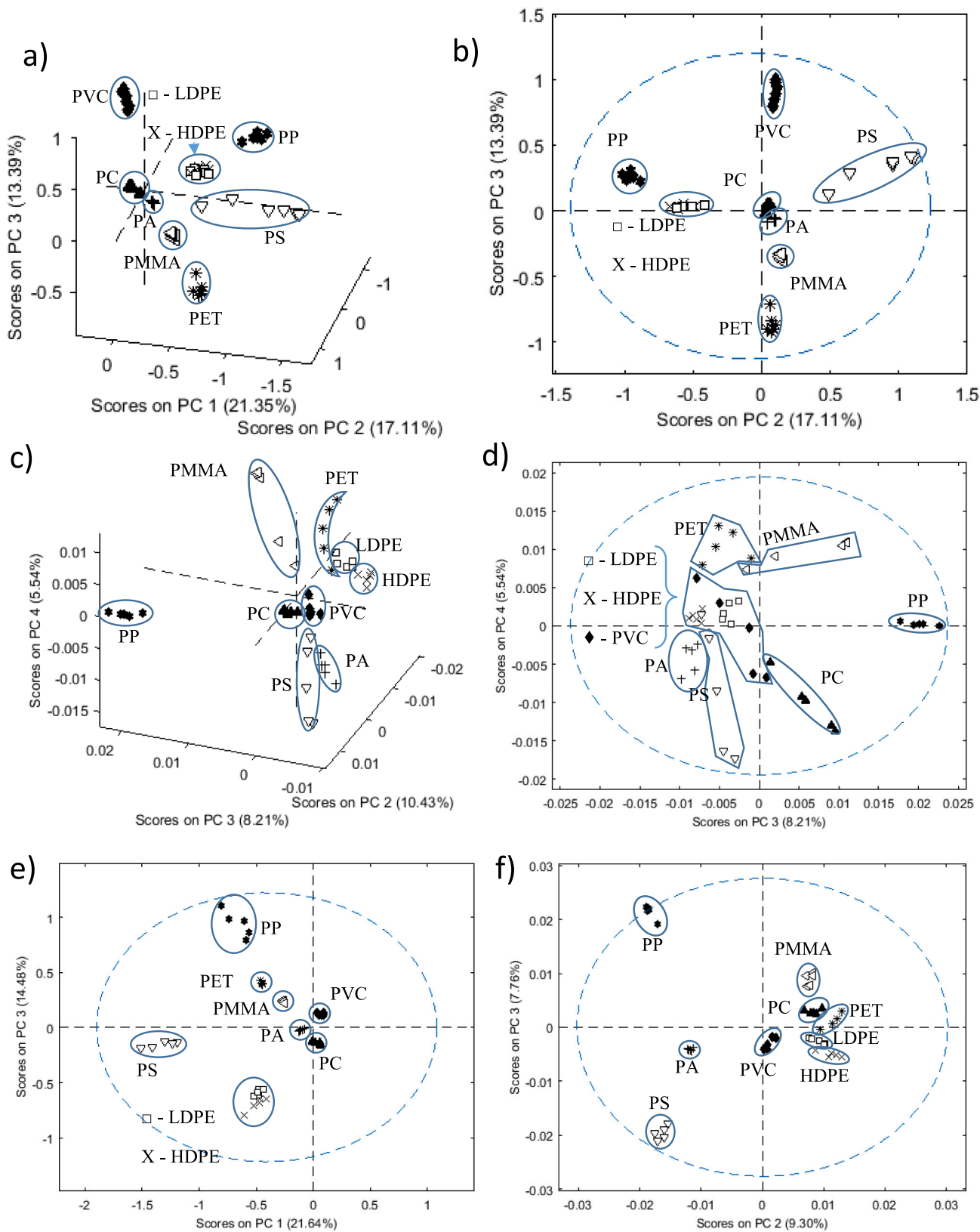
Fig. 6. Representation of the most relevant principal component subspaces to identify the groups of polymers. Seawater-aged powder measured by micro reflectance (a) and (b); and by ATR (c) and (d). Dry-aged powder measured by micro reflectance (e) and ATR (f).

PC3 separates mainly PVC (highest positive scores) from PET (highest negative scores), Fig. 6a and b. The loadings reflect also this point (Fig. SM6) as PET is characterized by positive loadings, mainly C=O stretch. On the contrary, PVC –an essentially linear structure- is reflected in the most relevant negative loadings, including the typical C—Cl bending.

The variables associated to those loadings were not enough to differentiate the groups of samples when a dedicated PCA was done, likely because of the complexity of the loadings (Fig. SM6) which make it hard any reasonable manual selection. However, after using SVM with these wavenumbers an acceptable separation of the polymers was found.

Using the dynamic PCA algorithm it was possible to reduce the amount of wavenumbers to 11: 2849, 2292, 1745, 1740, 1660, 1443, 1287, 1257, 905, 737 and 702 cm^{-1}. Finally, CART required 8 divisions (16 branches) to get a good separation of the polymers (Fig. SM7) using only 7 variables (i.e., 1800 (twice), 1787, 1776, 1743, 1507, 1392, and 1106 cm^{-1}).

The results obtained when ATR spectra were used are depicted in Fig. 6c and d. The PC2-PC3-PC4 scores subspace (24.1 % explained information) was chosen. Even though the groups appear quite separated from each other the results are not as good as for the study above using micro reflectance because the groups presented quite large dispersions (in fact, PC1 was not selected because the samples there become even more disperse, making it impossible to discern the groups). It also happens that the interpretation of the loadings is not straightforward. In PC2 (10.43 % explained variance) the only polymers that are sharply separated are PA and PP and HDPE and LDPE (figure not shown). The most important positive loadings for this factor (Fig. SM8) characterize HDPE and LDPE, whereas the negative loadings correspond to typical PA spectral bands.

PC3 (8.2 % explained variance) allows a slight separation of HDPE and LDPE (although they overlap with other polymers, Fig. 6c and d) and it clearly differentiates PP. The most important loadings that differentiate it from the other polymers (Fig. SM8) are linked to the C—H structures (positive loadings). The negative loadings point towards the other more complex structures with C=O groups.

PC4 (5.5 % explained variance) separates PET and PMMA (positive scores) from PC and PS (negative scores), Fig. 6d, though the groups are highly dispersed. The latter polymer becomes differentiated by the C=O stretching and the CH out-of-plane aromatic ring stretching (positive loadings, see Fig. SM8).

As for the micro reflectance spectra, the use of the variables associated to the most relevant loadings alone yielded bad results when a PCA was made and that was attributed to the difficulty in selecting the most relevant wavenumbers. However, applying SVM to these variables all the samples became well classified except for some LDPE ones.

On the other hand, using dynamic PCA it was possible to reduce the total amount of wavenumbers required to visualize the groups to 36, in the 2950–2840, 1780–1738 cm^{-1} ranges and 1535, 1427–1424 955–953, 829, 828, 725–723 cm^{-1} wavenumbers.

CART required only 10 divisions (20 branches) to get a good separation of the polymers (Fig. SM9) with only 9 variables (i.e., 1800 (twice), 1795, 1740, 1677, 1651, 1474, 1468, 1465 and 600 cm^{-1}), all of them in the surroundings of the typical C=O carbonyl region –as it happened with dynamic PCA, but for the 600 cm^{-1} wavenumbers.

3.4. Powder weathered under dry conditions

In essence, powdered samples weathered in dry conditions and measured by micro reflectance spectrometry behaved as their seawater-aged counterparts. In this case the separation between the polymers can be achieved with just two principal components (Fig. 6e); i.e. the PC1-PC3 subspace (ca. 36.5 % explained variance). PC2 was not selected because some PP samples got intertwined with those from HDPE and LDPE, yielding worst results. It was found that a PMMA sample behaved anomalously, so it was excluded from the final studies. There, PC1

(21.64 % variance) differentiates PS (extreme negative scores, Fig. 6e). The negative loadings influencing this factor the most were related to PS (Fig. SM10). The peak at 2924 cm^{-1} has no clear assignment and it may be a mixture of the C—H aromatic stretching from PS and the aliphatic CH stretching of HDPE and LDPE.

PC3 (ca. 14.5 % variance) in essence opposes PP (positive scores) to HDPE and LDPE (negative scores), with all other polymers showing close-to-zero scores, although each polymer forms very tight clusters, regardless of the degree of weathering during the study (Fig. 6e). The most important loadings are positive (Fig. SM10), but they cannot be associated to specific structures.

Dynamic PCA reduced the number of variables needed to visualize the groups of polymers from 3400 to 15 ones: 3457–3455, 2918, 1917, 1775, 1732, 1731, 1636–1634, 1269, 1268, 698 and 697 cm^{-1}. Using SVM with the wavenumbers associated with the highest loadings an acceptable separation among the polymers was obtained. Finally, CART employed only 9 divisions (18 branches) to get a good separation of the polymers (Fig. SM11) with only 8 variables (i.e., 1800 (twice), 1713, 1507, 1414, 1276, 1245, 1155 and 717 cm^{-1}).

Finally, two components separate the polymers when ATR spectra are considered (Fig. 6f): PC2 and PC3, being PC1 useless for this purpose. PC2 (9.3 % explained variance) opposes PA, PP and PS (negative scores) to the other polymers, most notably HDPE, LDPE, and PET (Fig. 6f), as it happened previously with the micro reflectance measurements. Relevant positive loadings for this factor (Fig. SM12) coincide with typical HDPE and LDPE bands (Fig. SM12) while highest negative loadings correspond mainly to PP.

PC3 (7.8 % explained variance) separates clearly PS and PP, Fig. 6f. The PS-related negative loading at 695 cm^{-1} (aromatic CH out-of-plane bending) opposes to the most relevant positive loadings (typical C—H stretching, likely from PP, ca. 2950 cm^{-1}, Fig. SM12).

Dynamic PCA required only 3 variables to visualize the groups, corresponding to the C—H stretching region (i.e., 2924, 2923 and 2922 cm^{-1}).

Combining SVM with the wavenumbers associated with the highest loadings a perfect differentiation between the polymers were obtained. Finally, CART made 9 divisions (18 branches) to get a good separation of the polymers (Fig. SM13) with 8 variables (i.e., 1800, 1659, 1605, 1468, 1467, 1136, 722 and 600 (twice) cm^{-1}).

3.5. General comparison of the selected wavenumbers

The wavenumbers selected by the different approaches were highly consistent among them, of course with the logical small differences due to their different fundamentals, and they allowed differentiating among the polymers at the model development (or training) stage. Fig. SM14 depicts graphically all the variables selected from the different models studied above (recall that SVM does not select variables by itself, but we included here a previous step that chooses those linked to the most relevant loadings). The figure shows clearly that the most relevant wavenumbers accumulate almost always in the fingerprint and the C—H stretching (~2800–3000 cm^{-1}) regions. Note that even despite CART considered only the fingerprint region, the variables selected for the decision nodes agree very well with the variables selected (in that region) using the other techniques.

The main question now is to decide which option is best. This involves a twofold choice: it has to be decided among ATR and reflectance measurements, and among the variable selection strategies. Unfortunately, this is a complex decision because although a variable might be useful do separate some polymers using (e.g.) ATR it might be detrimental when reflectance is considered. So, it is not only about ATR or reflectance, it is also about which particular combination of wavenumbers is considered. Many models discussed in the previous section had no false positives nor false negatives (detailed statistics are not show here) but one has to be aware that this may be an "artefact" caused by overfitting the models. Therefore, it is critical to test each and every

model with samples not used to develop the models at all. This is done in the next section.

3.6. Model validation

To validate the models, two set of samples were used, as detailed in Section 2.1; one considers particles extracted from the weathering setup during the period under study and the other considers field plastics collected at beaches. The latter are much more complex because of their unknown weathering extent, physical and chemical degradation, amount of additives, morphology, etc. Because of that, and after preliminary assays, the "HDPE" and "LDPE" categories will be combined into one, with the general denomination "PE".

PCA projection of the field samples into the scores subspace didn't yield satisfactory identifications, so it will not be considered further. This is explained because PCA and dynamic-PCA are not true classification methods as the final assignations are made subjectively, as per visual observation of the location of the samples. Hence, they are fast, although rough approaches to ascertain a polymer type. However, using the loadings from the PCA models it was possible to develop useful SVM models with a reduced number of variables Tables 1 and 2.

Table 1 presents the validation statistics for the SVM models. For the samples weathered artificially the results are encouraging for both spectrometric techniques. Micro reflectance models are, in general, slightly better than their ATR-based counterparts since 29 models (out of 30) had MCCs ≥0.8 (this happened for 26 ATR ones), with almost no false positives and with only one model showing poor classification

capabilities. The worst models were found for PMMA measured by ATR, although those developed using powders became slightly better than those for pellets. In general, the models differentiate the polymers really well.

When field samples are considered (Table 1, bottom part) the final assignations are not so satisfactory because the spectra became affected more by the different weathering processes they might had undergone: biofouling, physical erosion, chemical degradation, etc. Their spectra are noisier, with broader and less defined bands. Most field samples (>90 %) were thin sheet fragments, from food and one-use wrappings. This produces detrimental effects in reflectance measurements, as it often provokes an etalon-like effect: sinusoidal waves along the spectrum produced by the light passing through several parallel surfaces, which complicates the characterizations. This is reflected in the poor polymer identifications in the micro reflectance models, none of them surpassing a 0.5 MCC value. However, the ATR models showed more acceptable identifications, most of them having MCCs ≥0.8 (7 models out of 10), and low ratios of false positives and negatives. This seems very good news for garbage and plastic litter monitoring because they usually concentrate on relatively 'big' fragments, mostly when following OSPAR recommendations.

CART yielded less satisfactory models than SVM (Table 2), as evidenced by slightly worse statistics. For artificially weathered samples, reflectance-based models are preferred to ATR-based ones because up to 18 models lead to satisfactory ≥0.8 MCC values (vs. only 12 satisfactory ones using ATR). However, figures for field samples are not adequate. In our view, this might be because of the simple classification strategy of

Table 1
Validation statistics obtained for SVM models. The first value is the MCC statistic; those within the parenthesis represent the ratios of false positives and negatives (respectively). The colors in the boxes indicate the success of the model, from green (adequate model) to orange (unsuccessful model). (PVC was not available in pellets).

Weathered samples							
	ATR				Reflectance		
Polymer	Pellets		Powder		Pellets		Powder	
	Sea	Dry	Sea	Dry	Sea	Dry	Sea	Dry
PE	1 (0 ; 0)	1 (0 ; 0)	1 (0 ; 0)	1 (0 ; 0)	1 (0 ; 0)	0.8 (0.1 ; 0)	1 (0 ; 0)	0.9 (0.03 ; 0)
PA	1 (0 ; 0)	1 (0 ; 0)	0.9 (0 ; 0.3)	0.7 (0 ; 0.5)	1 (0 ; 0)	0.8 (0 ; 0.4)	1 (0 ; 0)	0.9 (0.03 ; 0)
PC	1 (0 ; 0)	0.9 (0 ; 0.3)	1 (0 ; 0)	0.9 (0 ; 0.3)	1 (0 ; 0)	1 (0 ; 0)	1 (0 ; 0)	1 (0 ; 0)
PET	1 (0 ; 0)	1 (0 ; 0)	0.9 (0 ; 0.3)	0.9 (0.03 ; 0)	1 (0 ; 0)	1 (0 ; 0)	0.9 (0 ; 0.2)	1 (0 ; 0)
PMMA	0.5 (0. ; 0.8)	0.7 (0 ; 0.5)	1 (0 ; 0)	0.7 (0 ; 0.5)	1 (0 ; 0)	1 (0 ; 0)	1 (0 ; 0)	0.8 (0 ; 0.4)
PP	0.9 (0 ; 0.3)	1 (0 ; 0)	1 (0 ; 0)	1 (0 ; 0)	0.9 (0 ; 0.2)	0 (0 ; 1)	1 (0 ; 0)	1 (0 ; 0)
PS	1 (0 ; 0)	1 (0 ; 0)	1 (0 ; 0)	0.9 (0 ; 0.3)	1 (0 ; 0)	1 (0 ; 0)	1 (0 ; 0)	0.9 (0 ; 0.2)
PVC	--	--	1 (0 ; 0)	0.9 (0 ; 0.3)	--	--	1 (0 ; 0)	0.9 (0 ; 0.2)

Field samples				
	ATR		Reflectance	
Polymer	Sea	Dry	Sea	Dry
PE	0.95 (0 ; 0.07)	0.95 (0 ; 0.07)	0.4 (0 ; 0.7)	0.3 (0.5 ; 0.1)
PET	0.8 (0.03 ; 0.2)	0.9 (0.02 ; 0.1)	0.3 (0 ; 0.9)	0.3 (0 ; 0.9)
PP	0.8 (0 ; 0.3)	0.8 (0 ; 0.3)	0.5 (0 ; 0.7)	0 (0 ; 1)
PS	0.8 (0 ; 0.5)	0.5 (0.07 ; 0.25)	0 (0 ; 1)	−0.04 (0.06 ; 1)
PVC	0.4 (0,02 ; 0.7)	0.6 (0 ; 0.6)	0.5 (0.02 ; 0.7)	0.5 (0.02 ; 0.7)

Table 2

Validation statistics obtained for CART models. The first value corresponds to the MCC statistic; those within the parenthesis represent the ratios of false positives and negatives (respectively). The colors in the boxes indicate the success of the model, from green (adequate model) to orange (unsuccessful model). (PVC was not available in pellets).

	Weathered samples							
	ATR				Reflectance			
Polymer	Pellets		Powder		Pellets		Powder	
	Sea	Dry	Sea	Dry	Sea	Dry	Sea	Dry
PE	1 (0 ; 0)	0.9 (0.2 ; 0)	0.9 (0 ; 0.1)	0.9 (0 ; 0.1)	0.3 (0.6 ; 0.2)	0.6 (0.5 ; 0.1)	0.9 (0 ; 0.1)	0.9 (0.1 ; 0)
PA	0.85 (0 ; 0.3)	0.7 (0 ; 0.5)	0.2 (0.7 ; 0.8)	0.3 (0.7 ; 0.5)	0.6 (0 ; 0.6)	0 (0 ; 1)	0.9 (0.2 ; 0)	1 (0 ; 0)
PC	1 (0 ; 0)	0.9 (0 ; 0.3)	0.5 (0 ; 0.8)	0.7 (0.4 ; 0)	0.8 (0 ; 0.4)	0.4 (0 ; 0.8)	0 (0 ; 1)	0.9 (0.2 ; 0)
PET	0 (0 ; 1)	−0.07 (1 ; 1)	0 (0 ; 1)	0.7 (0.3 ; 0.3)	1 (0 ; 0)	0.8 (0.4 ; 0)	0.8 (0.4 ; 0)	0 (0 ; 1)
PMMA	−0.06 (1 ; 1)	0.5 (0.6 ; 0.3)	1 (0 ; 0)	0.5 (0 ; 0.75)	0.4 (0 ; 0.8)	0.8 (0 ; 0.4)	0.2 (0.7 ; 0.6)	0.6 (0.2 ; 0.5)
PP	0.5 (0.7 ; 0)	0.8 (0.3 ; 0)	0.9 (0.3 ; 0)	−0.059 (0 ; 0)	0.1 (0.8 ; 0.8)	0.5 (0.5 ; 0.4)	0.9 (0.2 ; 0)	0.9 (0 ; 0.2)
PS	1 (0 ; 0)	0.9 (0 ; 0.3)	0 (0 ; 1)	0.5 (0.3 ; 0.5)	0.9 (0 ; 0.2)	0.8 (0.2 ; 0.2)	1 (0 ; 0)	0.9 (0 ; 0.2)
PVC	--	--	0.4 (0.8 ; 0)	0.7 (0 ; 4)	--	--	0.9 (0 ; 0.2)	0.9 (0.2 ; 0)

	Field samples			
	ATR		Reflectance	
Polymer	Powder		Powder	
	Sea	Dry	Sea	Dry
PE	0.4 (0.5 ; 0.2)	0.4 (0.5 ; 0.2)	0.3 (0.5 ; 0.2)	0.03 (0.6 ; 0.7)
PET	0.4 (0 ; 0.8)	0.6 (0.4 ; 0.4)	0.2 (0.5 ; 0.9)	0.1 (0.8 ; 0.8)
PP	0 (0 ; 1)	0.5 (0.2 ; 0.6)	−0.2 (1 ; 1)	−0.15 (0.9 ; 0.9)
PS	0 (0 ; 1)	−0.05 (1 ; 1)	0 (0 ; 1)	0.7 (0 ; 0.5)
PVC	0.4 (0.6 ; 0.3)	0.3 (0.6 ; 0.7)	0.4 (0.6 ; 0.3)	0.1 (0.8 ; 0.6)

the CART method. Dichotomic decision rules work well as long as similar spectra are considered for both calibration and validation. However, field samples were exposed to many weathering phenomena that, finally, distort the original spectrum so that the dichotomic absorbance decisions at the different nodes can be misleading.

Therefore, in the authors' opinion the final tradeoff analysis points out that ATR analysis (of both pellets and powders) combined with the chemometric support vector machine tool lead to the most satisfactory differentiation among the nine polymers considered in this work, along with satisfactory classification ratios of new samples. Although particular details were given in the previous sections, Table SM1 resumes the variables employed for each model and it can be seen that the three most relevant structural moieties involved in the differentiation and classification of the polymers were the C—H stretching, C—H bending, C═O stretching and the C—H out-of-plane bending (likely of aromatic rings); see Table SM2 (compiled from Brandon et al. (2016), Tiwari et al. (2019), Vasanthan (2012), Veerasingam et al. (2021), Jung et al. (2018)). Somehow this suggests that the models try to find out the signals of the main structural chains of the polymers (note that –for instance- the broad O—H stretching band typical of polymer weathering in the 3000–3200 cm^{-1} region does not appear at all within any variable selection).

4. Conclusions

The results obtained in this study indicate that polymer weathering complicates the formation of clear groups of samples in multivariate studies. In many cases, high-order principal components were needed to visualize more or less definite groups. This means that the most relevant spectral variance is not related to the different polymers but to other factors, mostly weathering. In general, the micro reflectance spectra of pellets were more interpretable and lead to better groups than those of powders, likely because reflected radiation is mostly specular, which yields simpler spectra than the diffuse radiation from the powders.

The studies presented here suggest that pattern recognition models developed with a reduced suite of selected variables may be a good way to address this problem. All the variable selection strategies allowed for significant reductions in the number of wavenumbers required to visualize the groups of polymers; being the most extreme situation that for dynamic PCA in the dry weathering of powdered polymers by ATR which required only three wavenumbers to differentiate the groups.

The simplest feature selection implies selecting wavenumbers associated to the maximum loadings of the principal components. This yields satisfactory differentiations when the spectra are well defined, mostly with pellet configurations. When this option is combined with SVM it is possible to differentiate all polymers with only some few marginal errors in some models (mostly for HDPE and LDPE, due to their spectral similarity).

Dynamic PCA is also a very simple methodology and it leads to very satisfactory results although the number of wavenumbers required to visualize the groups of polymers vary among the assays. In most cases, only 10 wavenumbers (out of the 3400 initial ones) were sufficient. Unfortunately, the projections of the field samples led to poor assignations because they have to be done visually.

CART behaved very consistently and required around 8 wavenumbers to separate the polymer groups. However, they were not always 100 % homogeneous and results were not too satisfactory for field samples. This was attributed to the spectral differences between the field and artificially-weathered plastics (which in turn yielded good validations), which make the dichotomic CART decisions suboptimal for field

samples. The classification models for SVM are more satisfactory when ATR spectra are considered. In particular, SVM performed clearly better than CART for field samples.

In our view, this work opens up the possibility of identifying polymers is spite of their weathering level by considering a reduced number of IR wavenumbers, although more studies are needed to improve the modelization of tiny particles and to ascertain how to incorporate this approach into the databases.

A final reflection on the limitations and future work to refine this approach is in order. The artificial weathering process employed here yields physical and chemical degradation but biofouling was not considered. The SVM models worked well for field samples without obvious biofouling but it remains to be assessed whether they also work in other circumstances where more bio-materials are present at the surface of the plastics. Such a study is being done in our laboratory as a part of a more comprehensive project (the JPI-Oceans EU-funded MicroplasticX). As a referee pointed out, it also has to be studied how the models behave when big amounts of additives are added to the core polymer so that they affect its spectrum.

It is worth noting that this approach can be used for on-site field MPs identification. Right now there are commercial portable (car battery-powered) ATR-FTIR systems, even from major brands, and since they are controlled by laptops it is indeed possible to include the chemometric models there. However, micro reflectance instrumental systems are not still portable. So, currently the portability option depends on the size of the microplastics under scrutiny (likely, 500 μm would be the very minimum acceptable size for current ATR devices).

CRediT authorship contribution statement

Conceptualization: B.F.; J.M.A.; S.M.: Methodology, Software and Formal analysis: B.F.; J.M.A.; C. P-Q.; V.F-G.; Validation: B.F.; J.M.A.; V. F-G.; P. L-M.; S.M.; Resources and Funding acquisition: S.M.; P. L-M; Writing: B.F.; J.M.A.; C. P-Q.; V.F-G.; P.L-M.; S.M.

Declaration of competing interest

The authors declare the following financial interests/personal relationships which may be considered as potential competing interests: Prof. Dr. Soledad Muniategui reports financial support was provided by EU Framework Programme for Research and Innovation Societal Challenges. Soledad Muniategui reports financial support was provided by Spain Ministry of Science and Innovation. Soledad Muniategui reports financial support was provided by Government of Galicia Department of Culture Education and Universities.

Data availability

The authors do not have permission to share data.

Acknowledgments

Appendix A. Supplementary data

Supplementary data to this article can be found online at https://doi.org/10.1016/j.marpolbul.2022.113897.

References

Ali, S.S., Elsamahy, T., Koutra, E., Kornaros, M., El-Sheekh, M., Abdelkarim, E.A., Zhu, D., Sun, J., 2021. Degradation of conventional plastic wastes in the environment: a review on current status of knowledge and future perspectives of disposal. Sci. Total Environ. 771, 144719 https://doi.org/10.1016/j.scitotenv.2020.144719.

Andrade, J., Fernández-González, V., López-Mahía, P., Muniategui, S., 2019. A low-cost system to simulate environmental microplastic weathering. Mar. Pollut. Bull. 149, 110663 https://doi.org/10.1016/j.marpolbul.2019.110663.

Andrade, J.M., Ferreiro, B., López-Mahía, P., Muniategui-Lorenzo, S., 2020. Standardization of the minimum information for publication of infrared-related data when microplastics are characterized. Mar. Pollut. Bull. 154 https://doi.org/10.1016/j.marpolbul.2020.111035.

Arrieta, C., Dong, Y., Lan, A., Vu-Khanh, T., 2013. Outdoor weathering of polyamide and polyester ropes used in fall arrest equipment. J. Appl. Polym. Sci. 130, 3058–3065. https://doi.org/10.1002/app.39524.

Battaglia, P., Pedà, C., Musolino, S., Esposito, V., Andaloro, F., Romeo, T., 2016. Diet and first documented data on plastic ingestion of Trachinotus ovatus L. 1758 (Pisces: Carangidae) from the strait of Messina (central Mediterranean Sea). Ital. J. Zool. 83, 121–129. https://doi.org/10.1080/11250003.2015.1114157.

Bellas, J., Martínez-Armental, J., Martínez-Cámara, A., Besada, V., Martínez-Gómez, C., 2016. Ingestion of microplastics by demersal fish from the spanish Atlantic and Mediterranean coasts. Mar. Pollut. Bull. 109, 55–60. https://doi.org/10.1016/J.MARPOLBUL.2016.06.026.

Bläsing, M., Amelung, W., 2018. Plastics in soil: analytical methods and possible sources. Sci. Total Environ. 612, 422–435. https://doi.org/10.1016/J.SCITOTENV.2017.08.086.

Botterell, Z.L.R., Beaumont, N., Dorrington, T., Steinke, M., Thompson, R.C., Lindeque, P. K., 2019. Bioavailability and effects of microplastics on marine zooplankton: a review. Environ. Pollut. 245, 98–110. https://doi.org/10.1016/J.ENVPOL.2018.10.065.

Brandon, J., Goldstein, M., Ohman, M.D., 2016. Long-term aging and degradation of microplastic particles: comparing in situ oceanic and experimental weathering patterns. Mar. Pollut. Bull. 110, 299–308. https://doi.org/10.1016/j.marpolbul.2016.04.048.

Chamas, A., Moon, H., Zheng, J., Qiu, Y., Tabassum, T., Jang, J.H., Abu-omar, M., Scott, S.L., Suh, S., 2020. Degradation rates of plastics in the environment. Sustain. Chem. Eng. 8 (9), 3494–3511. https://doi.org/10.1021/acssuschemeng.9b06635.

Chiba, S., Saito, H., Fletcher, R., Yogi, T., Kayo, M., Miyagi, S., Ogido, M., Fujikura, K., 2018. Human footprint in the abyss: 30 year records of deep-sea plastic debris. Mar. Policy 96, 204–212. https://doi.org/10.1016/J.MARPOL.2018.03.022.

Coffin, S., Huang, G.-Y., Lee, I., Schlenk, D., 2019. Fish and seabird gut conditions enhance desorption of estrogenic chemicals from commonly-ingested plastic items. Environ. Sci. Technol. 53, 4588–4599.

Compa, M., Ventero, A., Iglesias, M., Deudero, S., 2018. Ingestion of microplastics and natural fibres in Sardina pilchardus (Walbaum, 1792) and Engraulis encrasicolus (Linnaeus, 1758) along the spanish Mediterranean coast. Mar. Pollut. Bull. 128, 89–96. https://doi.org/10.1016/j.marpolbul.2018.01.009.

Cuadros-Rodríguez, L., Pérez-Castaño, E., Ruiz-Samblás, C., 2016. Quality performance metrics in multivariate classification methods for qualitative analysis. TrAC - Trends Anal. Chem. 80, 612–624. https://doi.org/10.1016/j.trac.2016.04.021.

Fernández-González, V., Andrade-Garda, J.M., López-Mahía, P., Muniategui-Lorenzo, S., 2021a. Impact of weathering on the chemical identification of microplastics from usual packaging polymers in the marine environment. Anal. Chim. Acta 1142, 179–188. https://doi.org/10.1016/j.aca.2020.11.002.

Fernández-González, V., Andrade, J.M., Ferreiro, B., López-Mahía, P., Muniategui-Lorenzo, S., 2021b. Monitorization of polyamide microplastic weathering usigng attenuated total reflectance and microreflectance infrared spectrometry. Spectrochim. Acta, Part A 263, 120162. https://doi.org/10.1016/j.saa.2021.120162.

Fernández-González, V., Andrade-Garda, J.M., López-Mahía, P., Muniategui-Lorenzo, S., 2022. Misidentification of PVC microplastics in marine environmental samples. Trends Anal. Chem. 153, 116649 https://doi.org/10.1016/j.trac.2022.116649.

Gewert, B., Plassmann, M.M., Macleod, M., 2015. Pathways for degradation of plastic polymers floating in the marine environment. Environ. Sci. Process. Impacts 17, 1513–1521. https://doi.org/10.1039/c5em00207a.

Gok, A., Fagerholm, C.L., French, R.H., Bruckman, L.S., 2019. Temporal evolution and pathway models of poly(ethylene-terephthalate) degradation under multi-factor accelerated weathering exposures. PLoS One 14, 1–23. https://doi.org/10.1371/journal.pone.0212258.

Göpferich, A., 1996. In: Williams, D.F.B.T.-T.B.S.J.C. (Ed.), Mechanisms of Polymer Degradation and Erosion. Elsevier Science, Oxford, pp. 117–128. https://doi.org/10.1016/B978-008045154-1.50016-2.

ter Halle, A., Ladirat, L., Martignac, M., Mingotaud, A.F., Boyron, O., Perez, E., 2017. To what extent are microplastics from the open ocean weathered? Environ. Pollut. 227, 167–174. https://doi.org/10.1016/j.envpol.2017.04.051.

Hirsch, S.G., Barel, B., Shpasser, D., Segal, E., Gazit, O.M., 2017. Correlating chemical and physical changes of photo-oxidized low-density polyethylene to the activation

energy of water release. Polym. Test. 64, 194–199. https://doi.org/10.1016/j.polymertesting.2017.10.005.

Howell, E.A., Bograd, S.J., Seki, M.P., Polovina, J.J., 2012. On North Pacific circulation and associated marine debris concentration. Mar. Pollut. Bull. 65, 16–22. https://doi.org/10.1016/J.MARPOLBUL.2011.04.034.

Iñiguez, M.E., Conesa, J.A., Fullana, A., 2017. Microplastics in spanish table salt. Sci. Rep. 7, 8620. https://doi.org/10.1038/s41598-017-09128-x.

ISO, 2020. ISO/TR 21960:2020 Plastics — Environmental Aspects — State of Knowledge and Methodologies. ISO, Geneva (Switzerland).

Jenner, L.C., Rotchell, J.M., Bennett, R.T., Cowen, M., Tentzeris, V., Sadofsky, L.R., 2022. Detection of microplastics in human lung tissue using μFTIR spectroscopy. Sci. Total Environ. 831, 154907 https://doi.org/10.1016/j.scitotenv.2022.154907.

Jiang, J.-Q., 2018. Occurrence of microplastics and its pollution in the environment: a review. Sustain. Prod. Consum. 13, 16–23. https://doi.org/10.1016/J.SPC.2017.11.003.

Jung, M.R., Horgen, F.D., Orski, S.V., Rodriguez, C.V., Beers, K.L., Balazs, G.H., Jones, T.T., Work, T.M., Brignac, K.C., Royer, S.-J., Hyrenbach, K.D., Jensen, B.A., Lynch, J.M., 2018. Validation of ATR FT-IR to identify polymers of plastic marine debris, including those ingested by marine organisms. Mar. Pollut. Bull. 127, 704–716. https://doi.org/10.1016/J.MARPOLBUL.2017.12.061.

Koelmans, A.A., Mohamed Nor, N.H., Hermsen, E., Kooi, M., Mintenig, S.M., De France, J., 2019. Microplastics in freshwaters and drinking water: critical review and assessment of data quality. Water Res. 155, 410–422. https://doi.org/10.1016/J.WATRES.2019.02.054.

Lamb, J.B., Willis, B.L., Fiorenza, E.A., Couch, C.S., Howard, R., Rader, D.N., True, J.D., Kelly, L.A., Ahmad, A., Jompa, J., Harvell, C.D., 2018. Plastic waste associated with disease on coral reefs. Science (80-.) 359. https://doi.org/10.1126/science.aar3320, 460 LP – 462.

León, V.M., García-Agüera, I., Moltó, V., Fernández-González, V., Llorca-Pérez, L., Andrade, J.M., Muniategui-Lorenzo, S., Campillo, J.A., 2019. PAHs, pesticides, personal care products and plastic additives in plastic debris from spanish Mediterranean beaches. Sci. Total Environ. 670, 672–684. https://doi.org/10.1016/j.scitotenv.2019.03.216.

Leslie, H.A., Van Velzen, M.J., Brandsma, S.H., Vethaak, A.D., Garcia-Vallejo, J.J., Lamoree, M.H., 2022. Discovery and quantification of plastic particle pollution in human blood. Environ. Int. 163, 107199 https://doi.org/10.1016/j.envint.2022.107199.

Luo, H., Xiang, Y., Zhao, Y., Li, Y., Pan, X., 2020. Nanoscale infrared, thermal and mechanical properties of aged microplastics revealed by an atomic force microscopy coupled with infrared spectroscopy (AFM-IR) technique. Sci. Total Environ. 744 https://doi.org/10.1016/j.scitotenv.2020.140944.

Markic, A., Gaertner, J.-C., Gaertner-Mazouni, N., Koelmans, A.A., 2020. Plastic ingestion by marine fish in the wild. Crit. Rev. Environ. Sci. Technol. 50, 657–697. https://doi.org/10.1080/10643389.2019.1631990.

Mecozzi, M., Pietroletti, M., Monakhova, Y.B., 2016. FTIR spectroscopy supported by statistical techniques for the structural characterization of plastic debris in the marine environment: application to monitoring studies. Mar. Pollut. Bull. 106, 155–161. https://doi.org/10.1016/j.marpolbul.2016.03.012.

Oreski, G., Wallner, G.M., 2005. Aging mechanisms of polymeric films for PV encapsulation. Sol. Energy 79, 612–617. https://doi.org/10.1016/J.SOLENER.2005.02.008.

PlasticEurope, 2021. Plastics - The Facts 2021: An Analysis of European Plastics Production, Demand and Waste Data.

Prata, J.C., 2018. Airborne microplastics: consequences to human health? Environ. Pollut. 234, 115–126. https://doi.org/10.1016/J.ENVPOL.2017.11.043.

Primpke, S., Christiansen, S.H., Cowger, W., et al., 2020. Critical assessment of analytical methods for the harmonized and cost-efficient analysis of microplastics. Appl. Spectrosc. 74 (9), 1012–1047. https://doi.org/10.1177/0003702820921465.

Raddadi, N., Fava, F., 2019. Biodegradation of oil-based plastics in the environment: existing knowledge and needs of research and innovation. Sci. Total Environ. 679, 148–158. https://doi.org/10.1016/j.scitotenv.2019.04.419.

Renner, G., Schmidt, T.C., Schram, J., 2017. A new chemometric approach for automatic identification of microplastics from environmental compartments based on FT-IR spectroscopy. Anal. Chem. 89, 12045–12053. https://doi.org/10.1021/acs.analchem.7b02472.

Shi, Y., Liu, P., Wu, X., Shi, H., Huang, H., Wang, H., Gao, S., 2021. Insight into chain scission and release profiles from photodegradation of polycarbonate microplastics. Water Res. 195, 116980 https://doi.org/10.1016/j.watres.2021.116980.

Tiwari, M., Rathod, T.D., Ajmal, P.Y., Bhangare, R.C., Sahu, S.K., 2019. Distribution and characterization of microplastics in beach sand from three different indian coastal environments. Mar. Pollut. Bull. 140, 262–273. https://doi.org/10.1016/j.marpolbul.2019.01.055.

Van Cauwenberghe, L., Janssen, C.R., 2014. Microplastics in bivalves cultured for human consumption. Environ. Pollut. 193, 65–70. https://doi.org/10.1016/J.ENVPOL.2014.06.010.

Vasanthan, N., 2012. Crystallinity determination of nylon 66 by density measurement and fourier transform infrared (FTIR) spectroscopy. J. Chem. Educ. 89, 387–390. https://doi.org/10.1021/ed200398m.

Veerasingam, S., Ranjani, M., Venkatachalapathy, R., Bagaev, A., Mukhanov, V., Litvinyuk, D., Mugilarasan, M., Gurumoorthi, K., Guganathan, L., Aboobacker, V.M., Vethamony, P., 2021. Contributions of fourier transform infrared spectroscopy in microplastic pollution research: a review. Crit. Rev. Environ. Sci. Technol. 51, 2681–2743. https://doi.org/10.1080/10643389.2020.1807450.

Venkatachalam, S., Nayak, S.G., Labde, J.V., Gharal, P.R., Rao, K., Kelkar, A.K., 2012. Degradation and recyclability of poly (ethylene terephthalate). In: Polyester. InTech Rijeka, Croatia, pp. 75–98. https://doi.org/10.5772/48612.

Wang, J., Tan, Z., Peng, J., Qiu, Q., Li, M., 2016. The behaviors of microplastics in the marine environment. Mar. Environ. Res. 113, 7–17. https://doi.org/10.1016/J.MARENVRES.2015.10.014.

Wayman, C., Niemann, H., 2021. The fate of plastic in the ocean environment-a minireview. Environ Sci Process Impacts 23, 198–212. https://doi.org/10.1039/d0em00446d.

Wilcox, C., Puckridge, M., Schuyler, Q.A., Townsend, K., Hardesty, B.D., 2018. A quantitative analysis linking sea turtle mortality and plastic debris ingestion. Sci. Rep. 8, 1–11. https://doi.org/10.1038/s41598-018-30038-z.

Young, L.C., Vanderlip, C., Duffy, D.C., Afanasyev, V., Shaffer, S.A., 2009. Bringing home the trash: do Colony-based differences in foraging distribution Lead to increased plastic ingestion in laysan Albatrosses? PLoS One 4, e7623. https://doi.org/10.1371/journal.pone.0007623.

Yousif, E., Haddad, R., 2013. Photodegradation and photostabilization of polymers, especially polystyrene: review. Springerplus 2, 1–32. https://doi.org/10.1186/2193-1801-2-398.

Zhang, K., Hamidian, A.H., Tubić, A., Zhang, Y., Fang, J.K.H., Wu, Ch., Lam, P.K.S., 2021. Understanding plastic degradation and microplastic formation in the environment: a review. Environ. Pollut. 274, 116554 https://doi.org/10.1016/j.envpol.2021.116554.